ELSEVIER

Catalysis Today 41 (1998) 191–206

CATALYSIS TODAY

Spectroscopic characterization of the acid properties of metal oxide catalysts

Guido Busca*

Istituto di Chimica, Facoltà di Ingegneria, Università – P.le J.F. Kennedy, 16129 Genova, Italy

Abstract

The IR spectroscopic methods for the characterization of the surface acidity of metal oxide catalysts are briefly reviewed. The use of different basic probe molecules whose IR spectra are sensitive to protonation and/or to the strength of Lewis acid–base interaction is described. The results obtained for the characterization of the Lewis acid strength of more than 30 binary and ternary mixed oxides are interpreted on the basis of the different polarizing powers of the involved cations. The characterization of the Brønsted acidity of several oxides and zeolites made by using the ''basic strength method'', the ''hydrogen bonding method'' and the ''olefin polymerization method'' is also described. © 1998 Elsevier Science B.V. All rights reserved.

Keywords: Acidity; Metal oxides; FI-IR spectroscopy; Adsorption

1. The surface acido-basicity of metal oxides

1.1. Basic concepts

Acidity and basicity have been defined in different ways. According to the current status of the surface science of metal oxides, the most relevant definitions are the following:

1. According to the concepts independently proposed by J.M. Brønsted and T.M. Lowry in 1923, an acid is any hydrogen-containing species able to release a proton and a base is any species capable of combining with a proton. This definition does not exclusively imply water as the reaction medium. In this view acido-basic interactions consist in the equilibrium exchange of a proton from an acid HA to a base B giving rise to the conjugated base of HA, A^-, plus the conjugated acid of B, HB^+:

   $$HA + B = A^- + HB^+.$$

2. In the same year, 1923, G.N. Lewis first proposed a different approach. In this view, an acid is any species that, because of the presence of an incomplete electronic grouping, can accept a electron pair to give rise to a dative or coordination bond. Conversely, a base is any species that possess a non-bonding electron pair that can be donated to form a dative or coordination bond. The Lewis-type acid–base interaction can be depicted as follows:

   $$B + A =^{\delta+} B \rightarrow A^{\delta-}.$$

   This definition is completely independent from water as the reaction medium, and is more general

*Corresponding author. Tel.: +39 10 3536024; fax: +39 10 3536028.

PII S0920-5861(98)00049-2

than the former one. In terms of Lewis acidity, the Brønsted-type acid HA is the result of the interaction of the Lewis-type acid species H^+ with the base A^-.

According to the above definitions, Lewis-type acids do not correspond to Brønsted-type acids. On the contrary, Lewis basic species are also Brønsted bases.

1.2. *The acido-basicity and the surface of oxide catalysts*

Oxide catalysts are solid compounds of oxygen and one or more metal or semimetal elements. "True" metal oxides are composed by a metal and oxygen and are consequently characterized by an almost ionic bond. When pure, they are most commonly crystalline materials. The ideal surface of a metal oxide crystal is composed by crystal faces (exposed crystal planes), held together by corner and edges. The coordination of ions at the "ideal" surface is necessarily uncomplete with respect to the coordination in the bulk. Even more uncomplete is the coordination of atoms at corners or edges. Surface reconstruction certainly occurs in order to decrease the free energy of the atoms exposed at the surface, but coordinative unsaturation will in part remain. The surface ions can also react with species from the environment, again to decrease the free energy. However, partly uncoordinated metal cations and oxide anions lie at the surface of metal oxide crystals, even in these conditions. These ions can act as acids and bases, respectively, according to the Lewis definition. So that, Lewis acid sites (coordinatively unsaturated cations) and basic sites (oxide anions) are expected, and actually found, at the surface of ionic metal oxides.

The reversible interaction of water (always present in the environment) with such surfaces is in part dissociative, as shown below:

$$\blacklozenge M^{n+1}O^{2-} + H_2O = HO^-M^{n+}\,{}^-OH,$$

where ◆ indicates a coordinative unsaturation responsible for Lewis acidity, so that coordinatively unsaturated cations and anions can in part convert into surface hydroxy-groups. These groups are potentially Brønsted acidic, although they mostly behave as basic ^-OH groups, because the bond with which they are held to the metal cation is ionic (Scheme 1).

The oxides of semimetals, like silicon, boron, germanium, phosphorus, arsenic, and so on, are also

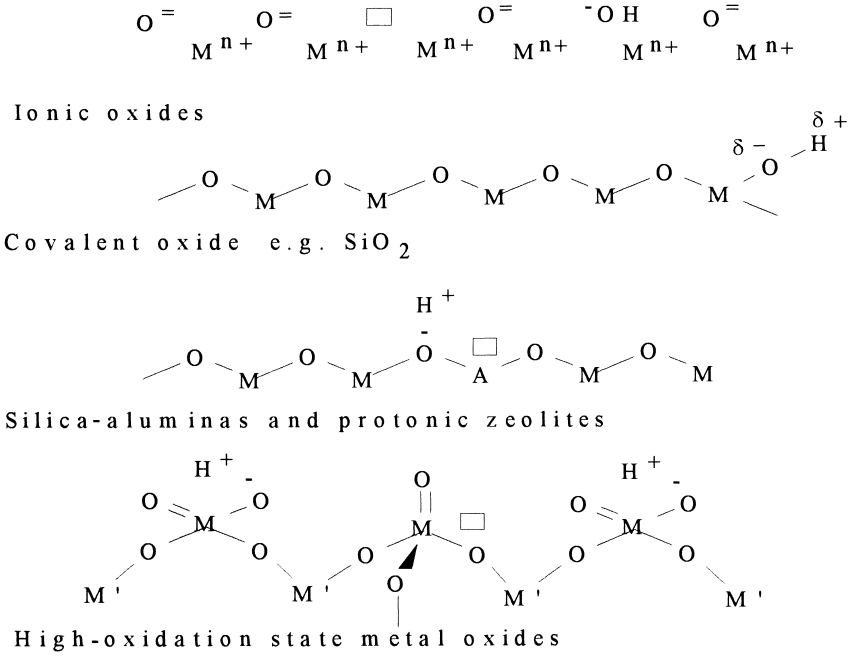

Scheme 1.

solids active or useful in catalysis. In this case the bond is essentially covalent. These materials can also be crystalline but not unfrequently amorphous. The surface of these materials can be modeled on the basis of the structure of a crystal plane like the surface that is generated when a particle is ideally cut along a plane to form two smaller particles. This would generate again coordinatively unsaturated element and oxygen atoms (or ions). However, the reactivity of these element atoms is so strong that they cannot stay as such in ''normal'' conditions. The elements of water saturate almost irreversibly the coordinative unsaturations, so that in this case Lewis acidity completely disappears and surface hydroxy-groups are formed, potentially responsible for Brønsted acidity.

In some cases, by ''doping'' covalent oxides with elements with lower valency (like Al in amorphous silica or crystalline silicalite, giving rise to silica-alumina or ZSM5 zeolite, respectively) a defect of charge is created, and this causes the formation of strong Brønsted acidity to balance it.

The oxides of metals in a high-oxidation state are also characterized by high covalency of the M–O bond, according to the high Sanderson's electronegativity of their ions. Accordingly, they show weak or no basicity. However, the cations tend to associate with some oxide ions giving rise to metal–oxygen ''double-bonds'' (vanadyl–, wolframyl–, molybdenyl– cations, etc.) whose coordination is very elastic. So, in spite of the covalency of metal–oxygen bonds, strong Lewis acidity can appear. The OH's are covalently bonded to the metal and the anion charge resulting from dissociation can be delocalized on terminal ''doubly bonded'' oxygens. Thus, medium to strong Brønsted acidity appears.

1.3. Spectroscopic detection of the surface acid sites: The method of the adsorbed probe-molecules

The IR and Raman spectroscopic detection of the surface acido-basic centers is based on the observation of the vibrational perturbation undergone by probe-molecules when they adsorb on them. Adsorption on ionic oxides mainly involves acido-basic interactions. Basic molecules adsorb on acid sites while acid molecules adsorb on basic sites.

1.3.1. Spectroscopic detection and characterization of the surface Lewis acid sites

As already cited, coordinatively unsaturated cations exposed at the surface of ionic oxides give rise to surface Lewis acid sites. Basic molecules can, consequently, interact with these sites by forming a new coordination bond, so completing or increasing the overall coordination at the surface cation. The stronger are the polarizing power of the Lewis acidic cation (charge to ionic radius ratio) and the basic strength of the adsorbate, the stronger is the Lewis interaction. Upon this interaction, electrons flow from the basic molecules towards the catalyst surface. This electronic perturbation as well as the molecular symmetry lowering arising from this contact are the causes of a vibrational perturbation of the adsorbate. In most cases, the vibrational perturbation only consists in shifts of the vibrational frequencies, the more pronounced, the stronger is the interaction, i.e. the greater is the Lewis strength of the surface site. Consequently, the shift of the position of some very sensitive bands of the adsorbate upon adsorption can be taken as a measure of the Lewis acid strength of the surface sites.

In Table 1, some data on the useful basic probe molecules are reported.

1.3.1.1. Adsorbed pyridine as a probe for Lewis acidity In spite of its toxicity, bad smell, low volatility and solubility in greases and rubber, giving rise to pollution of the vapor-manipulation ramps, pyridine is the most largely used basic probe molecule for surface acidity characterization [1–3]. The adsorption of pyridine on catalyst surfaces can give rise at least to the four adsorbed species reported in Scheme 2.

Species I is the product of the interaction of pyridine with Lewis acidic M cationic centers.

The pyridine molecule, C_5H_5N, is constituted by 11 atoms, so that 27 vibrational degrees of freedom ($3\times11-6$) correspond to vibrational modes. The usual notation of the vibrational modes of pyridine is derived from that of the parent molecule benzene, C_6H_6, which has one atom more and consequently three additional vibrational modes. The lower symmetry of pyridine (point group C_{2v}) with respect to benzene (point group D_{6h}) gives rise to the splitting of all doubly degenerate vibrational modes of benzene into two non-degenerate vibrational modes (Table 2). Almost all vibrational modes of the

Table 1
Basic probes, their pK_a's and the position of their diagnostic vibrational bands

Base		Conjugated acid	pK_a	PA[c]	Sensitive bands (base) Lewis acidity		Diagnostic band (acid) Brønsted acidity	
					Mode	Position[a]	Mode	Position [a]
Piperidine	$C_5H_{10}NH$	$C_5H_{10}NH_2^+$	11.1	933			δNH_2^+	∼1650
n-Butylamine	*n*-C_4H_9–NH_2	*n*-C_4H_9–NH_3^+	10.9				δ_{sym} NH_3^+	∼1540
Ammonia	NH_3	NH_4^+	9.2	846	$\delta_{sym}NH_3$	1300–1000	$\delta_{as}NH_4^+$	∼1440
Pyridine	C_5H_5N	$C_5H_5NH^+$	5.2	912	ν8a	1632–1580	ν8a	∼1640
					ν19b	1455–1438	ν19b	∼1540
					ν1(ring)	1020–990		
Acetone	$(CH_3)_2C{=}O$	$(CH_3)_2C{=}OH^+$	−7.2	816	νC=O	1730–1650		
Pivalonitrile	t-C_4H_9–C≡N	t-$C_4H_9C{\equiv}NH^+$	∼−10		νCN	2310–2235		
Acetonitrile	CH_3–C≡N	CH_3–$C{\equiv}NH^+$	−10.4	783	νCN	2340–2290		
					FR[b]	2315–2250		
Nitric oxide	NO	$[HNO]^+$			νN=O	2100–1875		
C monoxide	CO	$[HCO]^+$		598	νC≡O	2240–2150		

[a]Range cm^{-1}.
[b]Fermi resonance doublet.
[c]Proton affinity, Kcal/mol.

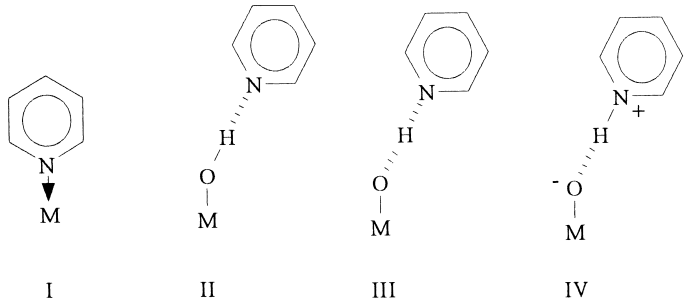

Scheme 2.

Table 2
Position (ν, cm^{-1}) of the vibrational bands of pyridine and pyridinium ion as compared to those of benzene

Point group D_{6h}				Point group C_{2v}					Assignments
Benzene C_6H_6							Pyridine C_5H_5N	Pyridinium $C_5H_5NH^+Cl^-$	
Sym	Notation	Act	ν (cm^{-1})	Notation	Sym	Act	ν (cm^{-1})	ν (cm^{-1})	
A_{1g}	1	R	992	1	A_1	IR,R	*991*	*1009*	νCC
E_{2g}	8	R	1596	8a	A_1	IR,R	*1583*	*1638*	νCC
				8b	B_1	IR,R	*1577*	*1608*	νCC
E_{1u}	19	IR	1479	19a	A_1	IR,R	*1481*	*1535*	νCC, δCC
				19b	B_1	IR,R	*1436*	*1485*	νCC, δCC

pyridine molecule, strongly coupled, are sensitive to the strength of the interaction involving its nitrogen lone pair. However, some of them are more sensitive than others. Accordingly, the 8a mode and the 19b mode (both mainly involving in-plane vibrations of the C_6 ring) are the most used in IR studies to evaluate

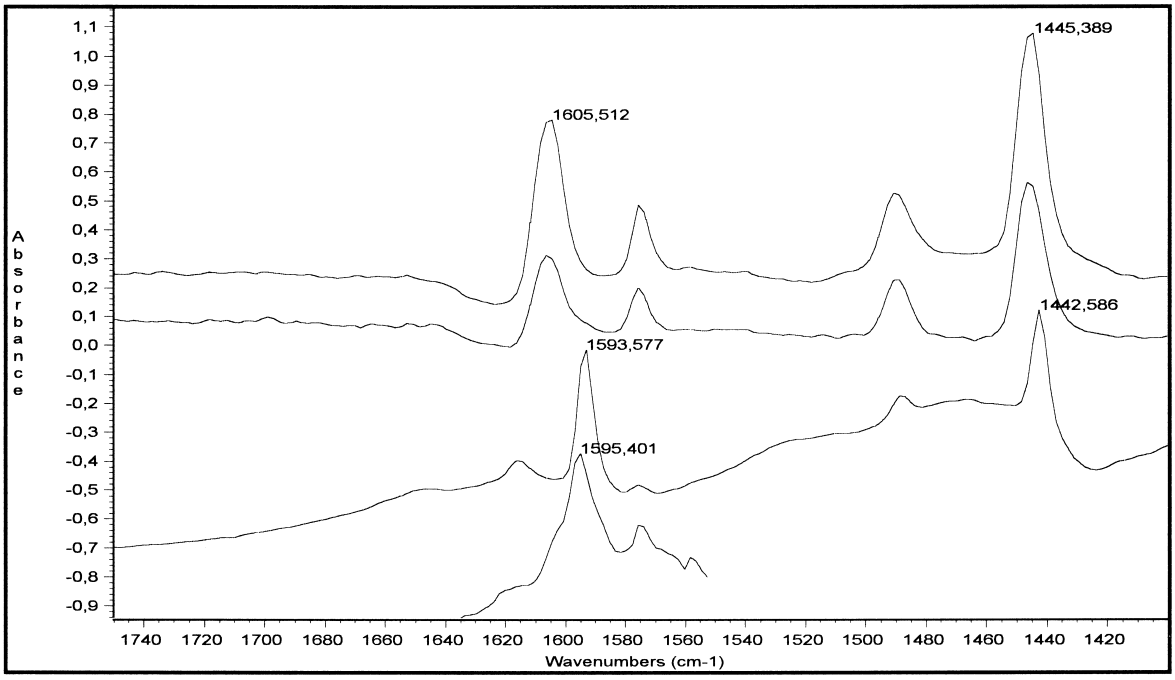

Fig. 1. The FT-IR spectra of adsorbed Lewis-bonded pyridine on four metatitanate compounds. From bottom to top: $SrTiO_3$ (cubic perovskite); $BaTiO_3$ (tetragonal perovskite); $NiTiO_3$ (ilmenite-type) and $CoTiO_3$ (ilmenite-type). The line-base for perovskite-type compounds is perturbed by adsorptions due to carbonate impurities. The region 1540–1350 cm^{-1} for $SrTiO_3$ is obscured. 8a and 19b bands are marked.

the strength of the Lewis acid sites (see Fig. 1). Raman spectroscopic studies are also performed on adsorbed pyridine. The 1 mode, weak in IR and frequently masked by skeletal absorptions, is very intense and accessible to Raman and is consequently used to characterize Lewis acidity with Raman spectroscopy of adsorbed pyridine. As shown in Table 2, some of the most sensitive bands of pyridine shift strongly (and also change of shape) when pyridine is protonated to form the pyridinium cation. This allows to distinguish coordinated from protonated pyridine easily. So, as it will be discussed further below, pyridine is largely used as a probe for both Lewis and Brønsted acidity [1].

In Table 3 the position of the most sensitive 8a mode of pyridine when coordinatively adsorbed on different oxide surfaces is reported. The position of this sharp band roughly correlates with the polarizing power of the adsorbant cation, PP, calculated as the charge to ionic radius ratio. In Table 3 some assumptions (mostly based on experimental data) have been made to improve this correlation. As for example, the adsorbing sites on CuO have been assumed to be monovalent Cu ions, according to the IR spectra of adsorbed CO that gave evidence of predominant monovalent Cu^+ adsorbing sites.

The correlation evident in Table 3 allows to draw some interesting conclusions:

1. On ABO_3 perovskite-type oxides the adsorbing site are assumed to be always the big A cation, the smaller B cation being likely not exposed at the surface. This leads to a significant difference in Lewis acidity between perovskite-type and ilmenite-type metatitanates. This difference can be deduced from Fig. 1, where it is seen that the 8a and 19b sensitive modes of adsorbed pyridine are both significantly shifted upwards in the ilmenites with respect to the perovskites.
2. In any case, in mixed oxides the counterions have always an effect. As for example, Ti and Zr cationic centers on the pyrophosphates are stronger Lewis

Table 3
Position (cm^{-1}) of the sensitive bands of adsorbed basic probe molecules on different catalyst surfaces (Lewis acid strength decreases from top to bottom)

Adsorbate	→	Pyridine	Ammonia	Pivalonitrile	Acetonitrile		Adsorbing site	
Mode	→	8a	$\delta_{sym}NH_3$	νC>N	νC>N[b]			
Surface↓	Structure↓				I	II	Type	PP
AlF_3	Crystalline	1627		2309-5			$_{IV}Al^{3+}$	7.7
γ-Al_2O_3	Def. spinel	1625	1295	2296	2330	2300	$_{IV}Al^{3+}$	7.7
		1615	1265				$_{IV}Al^{3+}$	
		1595	1220				$_{IV}Al^{3+}$	5.7
SiO_2–Al_2O_3	Amorphous	1622		2295			$_{IV}Al^{3+}$	7.7
$NiAl_2O_4$	Inv. spinel	1625					$_{VI}Al^{3+}$	7.7
		1605					$_{VI}Ni^{2+}$	2.8
		1595					$_{IV}Al^{3+}$	5.7
$MgAl_2O_4$	Norm. spinel	(1623)					$_{IV}Al^{3+}$	7.7
		1608					$_{IV}Mg^{2+}$	3.7
$ZnCr_2O_4$	Norm. spinel	1614					$_{IV}Zn^{2+}$	3.3
WO_3	Pseudocubic	1613	1275,1222				$_{VI}W^{6+}$	6.9[a]
γ-Fe_2O_3	Def. spinel	1612	1230				$_{IV}Fe^{3+}$	6.1
$MgFe_2O_4$	Inv. spinel	1612					$_{IV}Fe^{3+}$	6.1
		1606	1172				$_{VI}Fe^{3+}$	5.4
$ZnFe_2O_4$	Norm. spinel	1612					$_{IV}Zn^{2+}$	3.3
$(VO)_2P_2O_7$	Crystalline	1610		2290	2328	2300	VO^{3+}	5.5[a]
V_2O_5	Crystalline	1608	1249	2280	2324	2296	VO^{3+}	5.5[a]
ZrP_2O_7	Layered	1610			2321	2294	Zr^{4+}	5.0
TiO_2	Anatase	1610	1225	2285	2320	Mask	$_{V}Ti^{4+}$	
			1185	2260	2302	2274	$_{V}Ti^{4+}$	6.6
α-Fe_2O_3	Hematite	1608	1220,1180		2310	2283	$_{VI}Fe^{3+}$	5.5
$MTiO_3$[c]	Ilmenite-type	1605	1210				$_{VI}Ti^{4+}$	6.6
α-Cr_2O_3	Eskolaite	1608	1200				$_{VI}Cr^{3+}$	4.9
$MgCr_2O_4$	Norm. spinel	1607	1200				$_{VI}Cr^{3+}$	4.9
ZrO_2	Baddeleyite	1606	1210,1160				Zr^{4+}	∼5.0
$Mg_3(VO_4)_2$	Crystalline	1605			2295	2268	$_{VI}Mg^{2+}$	2.8
$LaMO_3$[a]	Perovskite-type	1602–1596					La^{3+}	2.8
α-Al_2O_3	Corundum	1597					$_{VI}Al^{3+}$	5.7
MgO	Periclase			2260	2307	2279	$_{IV}Mg^{2+}$	3.7
		1595			2294	2254	$_{VI}Mg^{2+}$	2.8
$BaAl_{12}O_{19}$	β-Alumina	1594					Ba^{2+}	1.4
$MTiO_3$[d]	Perovskites	1595-2					M^{2+}	1.8–1.4
CuO	Tenorite	1592					$_{VI}Cu^{+}$	1.0
K_2O–TiO_2	Anatase	1588	1143				K^{+}	0.7
Liquids		1583	1054	2236	2292	2254		

PP=polarizing power (charge to radius ratio).
[a]M=Fe, Cr, Mn, Co.
[b]I and II=Fermi resonance doublet.
[c]M=Co, Ni.
[d]M=Co, Ni.
[d]M=Sr, Ba.

acids than those on the corresponding oxides, and the acidity of Mg orthovanadate is intermediate between those of the pure oxides vanadia and magnesia.

3. It is still not clear why octahedral Al cations are so weakly acidic (α-Al_2O_3 is a very inert surface) with respect to octahedral Fe and Cr cations.

4. The Lewis acidity of WO_3 and V_2O_5-based catalysts does not correlate correctly with the others, because the polarizing power of W^{6+} and V^{5+} cations, calculated as above, is ''overestimated''. These values roughly correlate with the others if we calculate the polarizing power using the charge of wolframyl and vanadyl cations (WO^{4+} and VO^{3+}) and the radius of W^{6+} and V^{5+}.

The use of pyridine is also justified on the basis of its chemical stability on oxide surfaces. Transformation to α-pyridone on alumina and to dipyridyl on strongly activated alkali earth oxides and on oxidizing oxides only occurs at relatively high temperatures.

1.3.1.2. On the use of carbon monoxide and nitrogen monoxide as probes for the surface cationic centers

Carbon and nitrogen monoxides are very weak bases and are largely used for the surface characterization of cationic centers on metal oxide surfaces. The electronic structure of CO is described in Table 4 in correct terms [4] and in a simplified view. It implies a triple bond between C and O, according to the stretching frequency measured at 2143 cm^{-1} for the free molecule in the gas (see the rotovibrational absorption band in Fig. 2, left, bottom). In principle, the 14 electrons are distributed symmetrically between C and O atoms, so that the lower positive charge of the C nucleus with respect to O implies the formation of a dipole with the negative charge at the C atom, in spite of the lower electronegativity of C with respect to the O nucleus. For this reason, the CO molecule tends to interact through the C end with cationic centers (Scheme 3). This interaction is rather weak, usually completely reversible by outgassing at r.t. and should be studied at room or lower temperatures (e.g. at liquid nitrogen, 77 K).

Table 4
The electronic structure of carbon monoxide

Notation	Occup.		Simplified not.
6σ	—-	—	σ^*
2π	—-	—	$\pi_y^*\ \pi_z^*$
1π	↑↓	↑↓	$\pi_y\ \pi_z$
5σ	↑↓		σ
4σ	↑↓		C 2sp hybrid
3σ	↑↓		O 2sp hybrid
2σ	↑↓		C 1s
1σ	↑↓		O 1s

Table 5
CO stretching frequencies of carbon monoxide adsorbed at low temperature on closed shell cation oxides

Catalyst	νCO (cm^{-1})	Cation	PP
γ-Al_2O_3	2235, 2210	$_{IV}Al^{3+}$	7.7
	2200–2180	$_{VI}Al^{3+}$	5.7
TiO_2	2226, 2208, 2182	$_{VI}Ti^{4+}$	6.6
ZrO_2	2195, 2170	Zr^{4+}	~5.0
ZnO	2192, 2189	$_{IV}Zn^{2+}$	3.3
MgO	2158, 2149	$_{VI}Mg^{2+}$	2.8
La_2O_3	2155	La^{3+}	2.8
V_2O_5	—	No interaction	
Gas	2143		

According to theoretical calculations [5] this interaction is a simple polarization, with no formation of a true coordinative σ bond with the cationic center. This interaction tends to increase the CO bond order, so that the CO stretching frequency tends to increase upon it. Accordingly, the experimental measure of the CO stretching frequency for CO interacting with surface cations can be taken as a measure of the polarizing power of the cation or, in other terms, of its Lewis acidity (see Table 5).

However, when the cation or the metal atom contains, besides empty orbitals, also full or partly filled d-type orbitals, they can interact with the empty π^*-type orbitals of CO, via a π-type electron backdonation from the metal to CO. This implies that these antibonding orbitals become partly filled so that the bond order and the CO stretching frequency is decreased by this last interaction. In this case, the interaction can become very strong and very stable metal–carbonyl complexes can be formed. The experimental CO stretching frequency in this case is a complex function of the electron accepting power of the cation (Lewis acidity) and of its π-type electron donating power. Accordingly, the CO stretching frequency of CO adsorbed on several transition metal cations is very informative on the oxidation state of the adsorbing ion, but cannot be taken as a measure of its Lewis acidity. For this reason, the use of CO as a probe for surface acidity is limited to closed shell cation oxides (Table 5). The spectrum of CO adsorbed on TiO_2-anatase is shown in Fig. 2, left, top.

However, also some closed shell cations like V^{5+} and W^{6+} do not give rise to detectable adsorption. This allowed us to evaluate the coverage and the dispersion

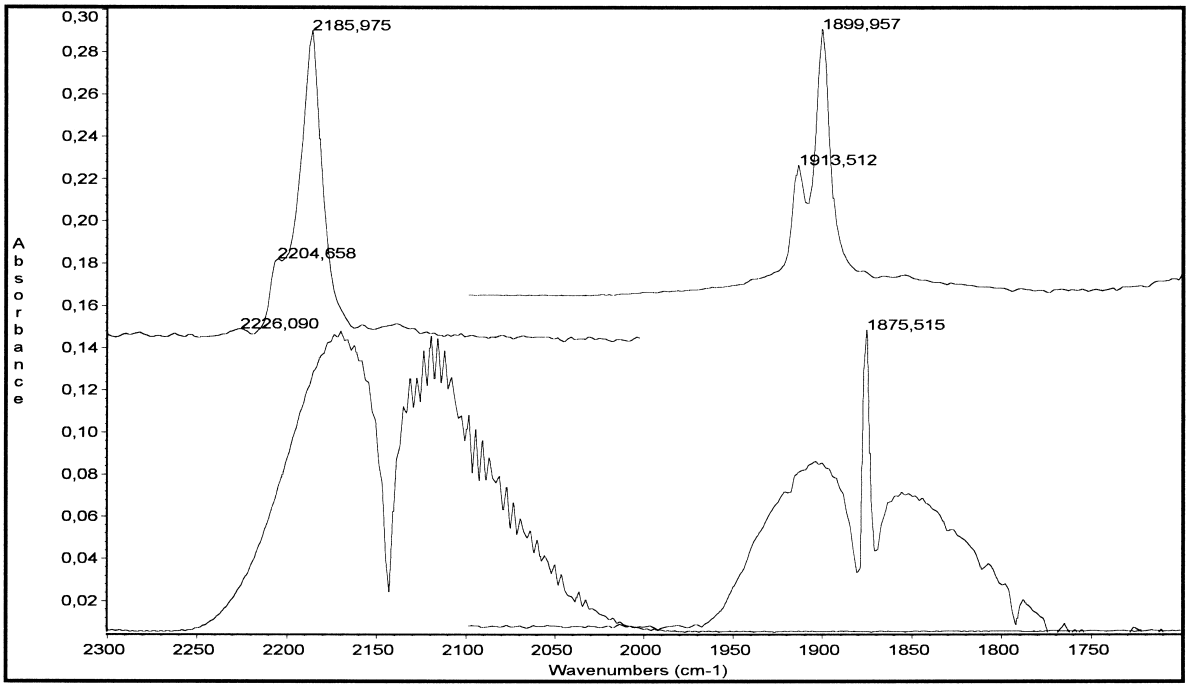

Fig. 2. FT-IR roto-vibrational spectra of gaseous CO (left, bottom) and NO (right, bottom), and FT-IR vibrational spectra of CO (left) and NO (right) adsorbed on TiO_2-anatase.

of the surface oxide species in V_2O_5–TiO_2 and WO_3–TiO_2 catalysts [6]. Zecchina and coworkers largely used CO as a probe of the surface sites in many oxide systems in relation to their morphology and sintering treatments. This work has been reviewed recently [7].

Nitrogen monoxide has one electron more than CO, so that the same electron configuration could apply with the additional electron in an antibonding π^*-type orbital. The bond order is decreased to 2,5 and this is reflected in the lower stretching frequency (1875 cm^{-1} for NO gas, see Fig. 2, right, bottom). Thus, the NO molecule is a radical and this makes its reactivity by far higher. It easily dimerizes to N_2O_2, is easily oxidized to NO^+, to nitrites NO_2^- or to NO_2, and is easily reduced to NO^- and to N_2O. NO can also easily disproportionate and is thermodynamically unstable towards decomposition to N_2+O_2. This makes this molecule very reactive so that its successful use as a probe for cationic centers is limited.

Anyway, NO can also interact with surface metal centers on metal oxides, giving rise to surface nitrosyl species. In homogeneous complexes, nitrosyl species can be either linear or bent (Scheme 3). Linear species generally form over cationic sites and are characterized by νNO higher than the gas [8], while bent nitrosyls are formed mainly over reduced centers and are characterized by νNO lower than the gas. In the former case the main interaction is between the N 2sp hybrid orbital and empty orbitals of the metal cation so that NO is depleted of electrons. The rise of the νNO frequency can be taken as a measure of the Lewis acidity of the adsorbing cation.

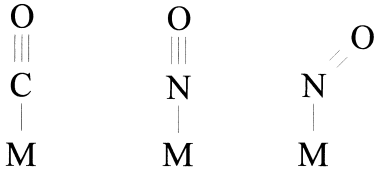

Scheme 3.

When the cation or the metal atom contains, besides empty orbitals, also full or partly filled d-type orbitals, they can interact with the π^*-type orbitals of NO

Table 6
Assignments of the bands of surface carbonyls and nitrosyls on TiO_2-anatase

CO adsorption			NO adsorption			Assignments
νCO	$\Delta\nu$CO	$\Delta\nu$CO/νCO	νNO	$\Delta\nu$NO	$\Delta\nu$NO/NO	
2226	+83	0.039	1935	+60	0.031	$_{IV}Ti^{4+}\leftarrow$CO
2205	+62	0.029	1913	+38	0.020	$_{V}Ti^{4+}\leftarrow$CO
2186	+43	0.020	1900	+25	0.013	$_{VI}Ti^{4+}\leftarrow$CO
2143			1875			Gases

molecule, via a π-type electron backdonation. This gives rise to bent nitrosyls, where N is likely sp^2 hybrid and the NO stretching frequency is decreased. In this case, the NO stretching frequency does not correlate with acidity.

In any case, sometimes a good correlation exists between the adsorbed species produced by contact with CO and NO. This is the case for TiO_2-anatase, as shown in Fig. 2. In both cases a main band is observed, with a smaller component at higher frequency and a third, very weak one, at very high frequencies. Possible assignments for such bands are reported in Table 6, where the subscripts indicate the overall coordination of the Ti cation after adsorption.

1.3.1.3. Other basic probes for the spectroscopic characterization of Lewis acidity Other basic probe molecules can be used for probing surface Lewis acidity. Other N-containing molecules, that are in water stronger bases than pyridine, like piperidine [9], *n*-butyl amine [10] and ammonia [11], can be successfully used too. However, they present in most cases, some disadvantages. Piperidine and *n*-butyl amine do not present very sensitive bands in a ''clean'' spectral region to be easily used to evaluate the basic strength. Ammonia can be very useful, although in some cases it is too reactive and gives rise to reactive adsorption. This is the case of its adsorption on aluminas, where a complex spectrum is obtained likely due to a disproportionation reaction like:

$$2NH_3 \rightarrow NH_4^+ + NH_2^-.$$

Moreover, the transformation of ammonia to amide species NH_2, imido-species, NH, and hydrazine species, NH_2–NH_2, as well as its oxidation to N_2, N_2^- and N_3^- species is well-documented [12]. To our experience, ammonia is a good probe for acidic non-oxidizing or poorly oxidizing surfaces [13].

The use of less basic organic probes like ketons and nitriles is also limited by their reactivity (enolization, polymerization, etc.). However, the spectroscopic features of the molecularly adsorbed species give rise to a picture that correlates quite well with what is obtained by pyridine and/or CO adsorption, as it can be deduced from Table 3. We largely used nitriles in acid catalysts characterization [6,14,15].

1.3.2. Spectroscopic detection of the surface Brønsted acid sites

The fragments arising from the dissociative adsorption of water on the surface of metal oxides give rise to hydroxy-groups that are potentially more or less active Brønsted acid sites. Such surface hydroxy-groups can be detected, directly, recording the IR spectra of the oxide catalyst powders in the region 3800–3000 cm^{-1}, where the O–H stretching modes (νOH's) fall. In Figs. 3 and 4 the spectra of the surface hydroxy-groups on some catalytic materials are reported, after outgassing. Although the position and shape of the νOH bands of such surface hydroxy-groups is informative on their coordination, these data do not give straightforward information on their Brønsted acidity. In fact, as for example, the position of the νOH band over a basic catalyst like MgO, of a weakly acidic catalyst as amorphous silica (both in Fig. 4, right) and of a strong Brønsted acidic catalyst like silica–alumina (Fig. 3) is almost the same (3745 ± 3 cm^{-1}). Moreover, very acidic catalysts like, for example, sulfated zirconia and titania (Fig. 4 left, for the latter) do not present any definite sharp νOH band, while others, like zeolite ZSM5 and silica–alumina, show sharp νOH bands (Fig. 3). These facts are due to two main reasons:

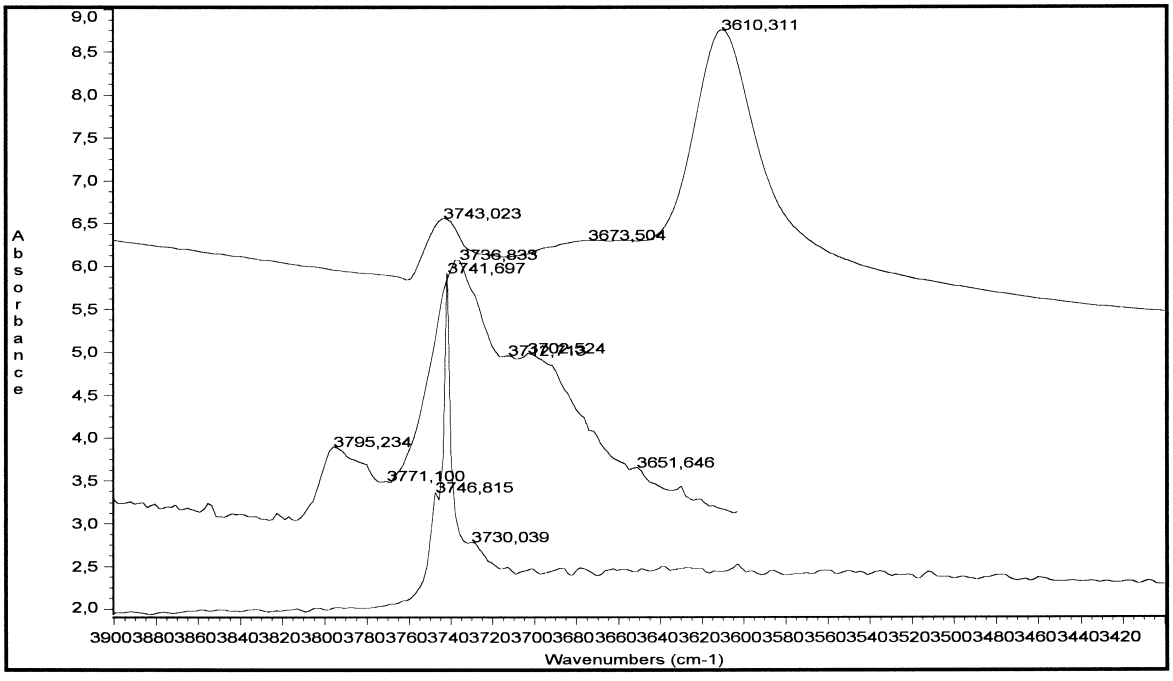

Fig. 3. FT-IR spectra of the surface hydroxy groups on zeolite ZSM5 (Engelhardt, top), γ-Al_2O_3 (Akzo, middle) and silica–alumina (Strem, bottom) after outgassing at 600°C (top), 700°C (middle) and 350°C (bottom).

1. The νOH frequency depends not only from the O–H bond strength, but also from the nature of the M–O(H) bond, i.e. from the element(s) to which the OH is bonded.
2. In any case, even for OH's bonded to the same element, the function νOH versus acidity is not necessarily linear but can present a maximum [16].
3. The state of the OH groups at the surface also depends on the basic strength of the oxide ions. In fact, in very covalent structures, like for silica alumina and zeolites, where oxygens are almost not basic, the acidic OH's are responsible for rather sharp and well-defined bands (Fig. 3) while when the nearest oxygen are more or less basic, the acidic OH's give rise to H-bondings, with a shift down and a broadening of the νOH band.
4. It seems also likely that the location of the acidic OH's inside a zeolite cavity can also be responsible for a shift down and broadening of the νOH band. This seems necessary to justify the location of the "acidic" OH band in zeolite HZSM5 at 3610 cm^{-1}, rather broad, with respect to the position of the "acidic" OH of amorphous silica–alumina at 3742 cm^{-1}, very sharp (Fig. 3).

1.3.3. *Spectroscopic characterization of the surface Brønsted acid sites*

1.3.3.1. The basic strength method The presence of Brønsted acid sites can be detected "indirectly" by studying the interaction of bases of appropriate strength and by monitoring the formation of the corresponding protonated species. This is done most frequently using again pyridine as the adsorbed probe molecule. On the titanates (Fig. 1) the 8a, 8b, 19a and 19b bands of coordinated molecular pyridine are observed, more or less shifted, as usual, towards higher frequencies. No traces are found of pyridinium cations. On the contrary, on GeP_2O_7 [17] the observed spectrum is definitely different, with a split broad band at 1640, 1628 cm^{-1}, another broad band at 1548 cm^{-1} and a very strong band at 1492 cm^{-1}. This spectrum is typical for pyridinium cations, as compared with the spectrum of pyridinium chloride (Table 2). According to these data we can

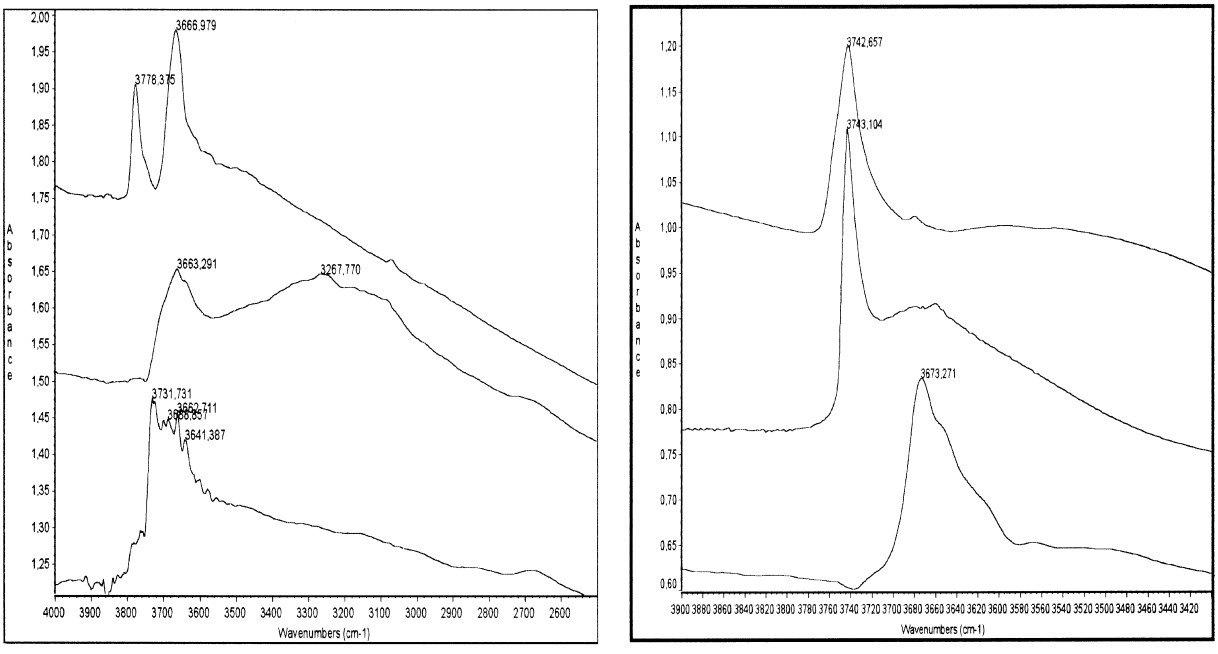

Fig. 4. FT-IR spectra of the surface hydroxy groups. left: ZrO_2 (tetr.) activated at 700°C (top); sulfated TiO_2 anatase activated at 400°C (middle); ''pure'' TiO_2-anatase activated at 400°C (bottom); right: MgO activated at 600°C (top), amorphous silica activated at 400°C (middle) and $ZnFe_2O_4$ activated at 400°C (bottom).

conclude that titania is a purely Lewis acidic material while GeP_2O_7 is a purely Brønsted acidic solid. Most frequently, solids can be both Lewis and Brønsted acidic. The interaction of pyridine with silica–alumina at r.t. gives rise to the spectrum shown in Fig. 5, top. The bands at 1597 and 1446 cm^{-1} are due to the 8a and 19b modes of pyridine molecules interacting via H-bonding with the weakly acidic surface hydroxy-groups of the catalyst (species II and/or III in Scheme 2) while the bands at 1623 and 1455 cm^{-1} are due to the same modes of pyridine molecularly coordinated on Al^{3+} cations, acting as Lewis acid sites (species I in Scheme 2).

The bands at 1639, 1547 and 1492 cm^{-1} are the most intense modes of pyridinium cations, associated to a total proton transfer from the Brønsted acidic surface OH group to the basic molecule (species IV in Scheme 2). According to these assignments, outgassing at 100°C causes the disappearance of the bands at 1597 and 1446 cm^{-1} (due to H-bonded pyridine), while the other, strongly held species are not perturbed. In Fig. 6 the spectra of the free surface OH groups on the silica–alumina sample after activation and in the presence of adsorbed pyridine are shown. The spectrum of the activated sample (top in Fig. 6) shows a sharp band at 3742 cm^{-1} with an evident component at 3747 cm^{-1}. This range is typical of the OH stretching of free silanol groups. In the conditions of Fig. 6, top (i.e. after contact with pyridine vapor and outgassing at r.t.) the component at 3742 cm^{-1} is almost completely disappeared, while a weaker and broad complex absorption with maxima near 3745, 3742 and 3735 cm^{-1} are apparent. Outgassing at 100°C causes only the very partial re-appearance of a component near 3740 cm^{-1}, now only slightly more intense than the highest frequency component, observed at 3745 cm^{-1}. We mention that in these conditions H-bonded pyridine is disappeared but pyridinium ions are still present, unaffected. This implies that the ''acid'' OH's responsible for the pyridine protonation and the less acidic OH's involved for H-bonding are both responsible for the band near 3741 cm^{-1}. The species responsible for the component at 3745–3747 cm^{-1} is either non-acidic or not

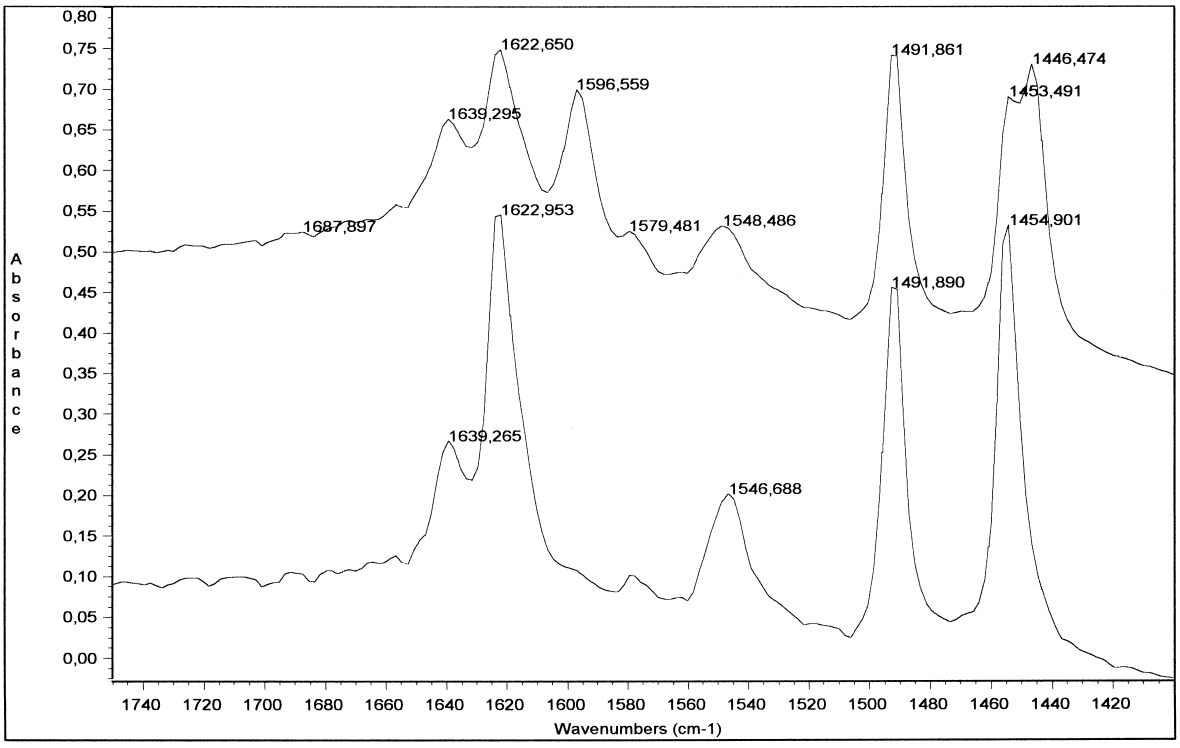

Fig. 5. FT-IR spectra of the suface species arising from adsorption of pyridine on a silica–alumina cracking catalyst (13% Al_2O_3 form Strem) at r.t. (above) and after outgassing at 100°C (below). Brønsted acidic. This is the case, for example, of silical–alumina, an active hydrocarbon cracking.

accessible. While on silica–alumina pyridine is partly protonated, on pure silica and on pure alumina it is not. The spectrum of pyridine adsorbed on γ-Al_2O_3 only shows bands typical of three different coordinated species (Fig. 7). However, stronger bases than pyridine can be protonated in part on alumina. In Fig. 7 the spectrum of piperidine adsorbed on γ-Al_2O_3 is also shown. The evident band at 1650–1610 cm^{-1} is absent in the spectrum of the "free" base and is due to the scissoring mode of the $–NH_2–$ group of dialkylammonium cations (in this case, piperidinium cations). Thus, the acid strength of the surface Brønsted sites on solid surfaces can be evaluated by the basic strength of the molecules they are able to protonate. In this respect, the question arises of whether the basic strength scale to be used is that applied in water solution (i.e. the pK_a scale) or in the gas phase (e.g. the proton affinity scale) which are not coincident (see Table 1). In particular it appears that in the gase phase pyridine is more acidic than ammonia, while the contrary is true in water. To our experiments, ammonia is more easily protonated than pyridine on oxide surfaces (see Table 7) so is apparently more basic.

1.3.3.2. The hydrogen-bonding method As discussed above, the strength of the acido-basic interaction depends on the acid strength of the acid as well as on the basic strength of the base. When the base is sufficiently strong, a Brønsted acid protonates it (species IV in Scheme 2), but when the base is too weak the interaction results in a hydrogen bonding (species II in Scheme 2). In intermediate cases, the proton transfer can be only partial so that a "symmetrical hydrogen bonding" occurs (species III in Scheme 2). These two situations can be detected and distinguished spectroscopically from protonation and interaction with Lewis sites. In fact, in both these cases the spectrum of the adsorbed base is only weakly perturbed with respect to the liquid, but in the same sense as for interaction with Lewis sites.

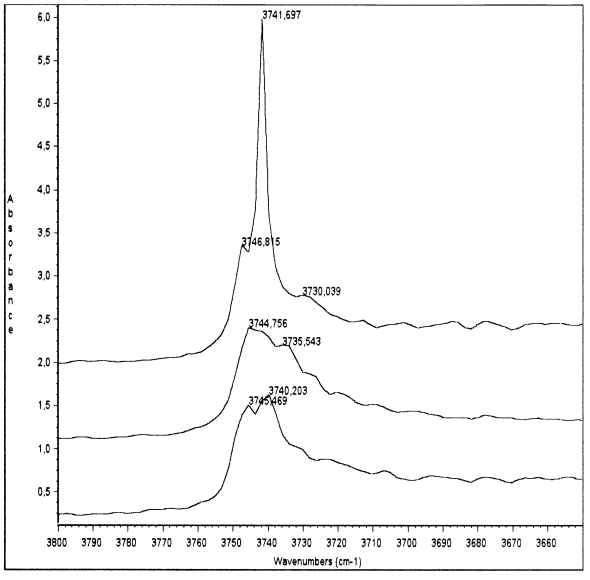

Fig. 6. FT-IR spectra of the surface hydroxy-groups of a silical–alumina cracking catalyst (13% Al_2O_3 from Strem) after activation at 350°C (top), after contact with pyridine vapor at r.t. (middle) and after outgassing at 100°C (bottom).

Moreover, hydrogen bonding causes the shift down and the broadening of the OH stretching bands of the surface OH groups. Simple hydrogen bonding gives rise to the formation of well-defined although broad OH stretching bands, and the shift of the maximum of the νOH band upon interaction can be taken as the H-bonding interaction. If the same base is used, this shift measures the acid strength of the protonic center. Very weak bases, that cannot ordinarily be protonated, like nitriles or benzene, can be used for this purpose. Low temperature adsorption of even weaker ''bases'', like CO or ethylene [18], are also useful experiments in this respect.

The formation of a stronger ''symmetrical'' hydrogen bonding causes the formation of an almost continuous absorption in the overall spectrum, giving rise to three maxima and two minima, the so-called ABC contour arising from Fermi resonance type interactions [19]. The minima correspond to the first overtones of the in plane, δOH, and the out of plane deformation modes, γOH, of the MOH group. This phenomenon occurs when the interaction of the base with the OH group is intermediate between H-bonding and a true Brønsted acid–base interaction.

An application of the hydrogen-bonding method to evaluate the Brønsted acid strength of the surface OH's on a catalyst is shown in Figs. 8 and 9, where the spectra of a H_3PO_4–SiO_2 catalyst (a model for ''solid phosphoric acid'') before and upon interaction with pivalonitrile are reported. This material shows two well-defined OH groups absorbing at 3743 and 3666 cm^{-1}, identified as SiOH and POH groups. Upon interaction with pivalonitrile, both hydroxy-groups are

Table 7
Evaluation of the Brønsted acid strength of surface hydroxy-groups on catalytic materials by different IR techniques

Catalyst	Protonation of					$\Delta\nu$OH nitriles	Behavior with *n*-butenes at r.t.	Polymerization of			
	AN	py	NH_3	RNH_2	Piper			Ethylene	Propene	Isobutene	1,3-butadiene
HZSM5	Yes	Yes	Yes	Yes	Yes	ABC	Polymerization+ isomerization	Yes	Yes	Yes	Yes
TiO_2–SO_4	No	Yes	Yes	Yes	Yes	ABC	Polymerization	Yes	Yes	Yes	Yes
Silica–alumina	No	Yes	Yes	Yes	Yes	ABC	Polymerization	No	Yes	Yes	Yes
H_3PO_4–SiO_2	No	Yes	Yes	Yes	Yes	ABC	Polymerization	No	No	Yes	Yes
AlF_3	No	(Yes)	Yes	Yes	Yes	>500					
B_2O_3–Al_2O_3	No	No	Yes		Yes	480–420, 330–280	Butoxide traces	No	No	Dimer	Yes
silicated-alumina	No	No			Yes	480–420, 330–280	$\Delta\nu$OH 200–300				
γ-Al_2O_3	No	No	Yes	Yes	Yes	450–400, 330–280	$\Delta\nu$OH 200–300	No	No	No	Yes
am-SiO_2	No	No	(Yes)	(Yes)		400	$\Delta\nu$OH 150–200	No	No	No	No
TiO_2-an.	No	No	No	No	No	<300		No	No	No	No
ZrO_2	No	No	No	No	No			No	No	No	No
MgO	No	No	No	No	No	~250		No	No	No	No

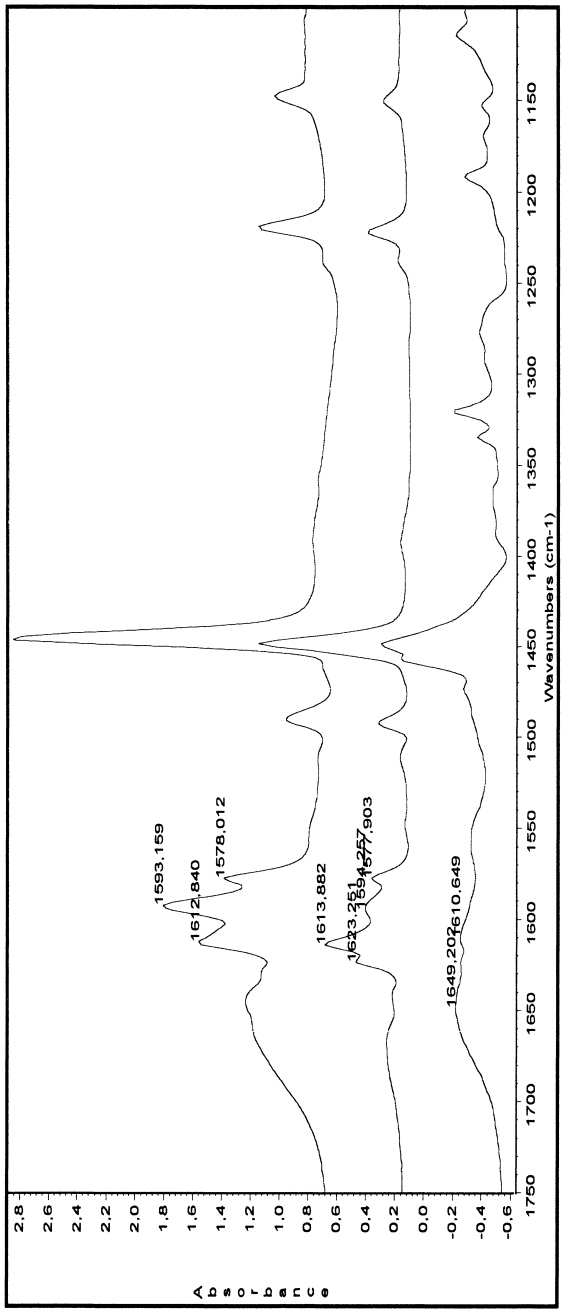

Fig. 7. FT-IR spectra of the adsorbed species arising from pyridine (top and middle) and piperidine (bottom) adsorption on γ-Al_2O_3 after otugassing at r.t. (top and bottom) and at 150°C (middle).

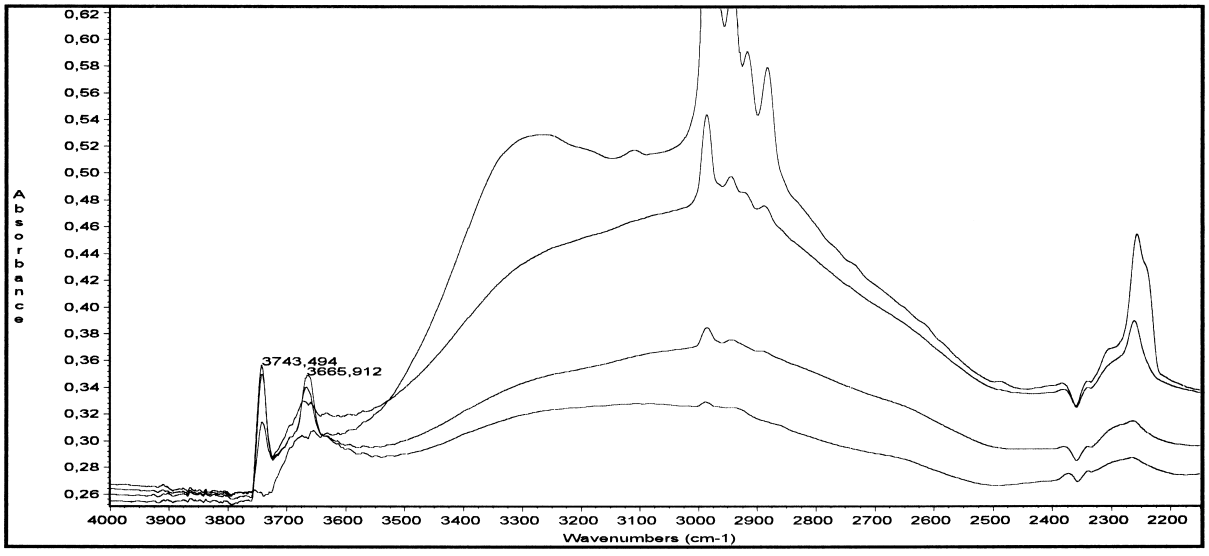

Fig. 8. FT-IR spectra of a H_3PO_4–SiO_2 catalyst after activation (a), contact with pivalonitrile vapor (b) and outgassing at room temperature (c) and at 100°C (d).

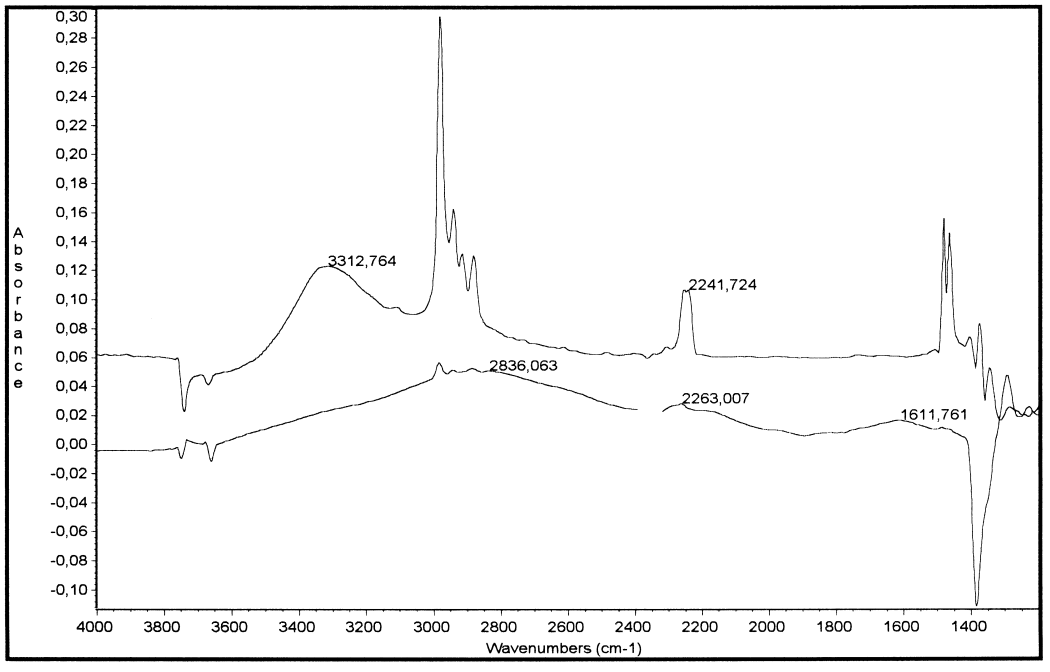

Fig. 9. Perturbation of the FT-IR spectrum of a H_3PO_4–SiO_2 catalyst upon contact with pivalonitrile; top: substraction spectra (a) and (b) of Fig. 8; bottom: substration spectra (c) and (d) of Fig. 8.

perturbed. However, the interaction with silanols is much weaker, being destroyed by outgassing at r.t. and giving rise to a well-defined νOH band centered at 3313 cm^{-1} (Fig. 9, top), i.e. with a shift of more than 400 cm^{-1}, like on amorphous silica (see Table 7). The CN stretching band of pivalonitrile upon interaction

with SiOH's only weakly shifts from 2236 (liquid phase value) to 2242 cm^{-1}. The interaction (Fig. 9, bottom) with POH's is much stronger and resists in part outgassing at 100°C. Moreover, this interaction gives rise to a more pronounced shift up of the νCN band of the adsorbate (to 2263 cm^{-1}) and to a ABC-type band contour, with maxima near 2835, 2200 and 1610 cm^{-1}, and minima near 2390 and 1900 cm^{-1}. This indicates that the δOH and γOH modes for POH interacting with pivalonitrile are located near 1195 and 950 cm^{-1}, respectively. Protonation of acetonitrile was found recently on HZSM5 [Trombetta et al. unpublished paper].

1.3.3.3. The olefin polymerization method Olefins and dienes are very reactive towards the electrophilic attack of Brønsted acid, and can undergo proton-catalyzed cationic polymerization. This phenomenon occurs the faster, the stronger is the Brønsted acid, the more electron-rich is the olefinic double bond and (in a low-temperature range) the higher is the temperature. Thus, the polymerization rate follows the order: 1,3-butadiene>isobutene>propene>ethylene. We previously used this set of olefin molecules to evaluate the Brønsted acidity of solid acids [20,21]. Very strong acids, like zeolite HZSM5, sulfated titania and zirconia, supported WO_3, cause the polymerization of ethylene at r.t. Less acid surfaces, like MoO_3–TiO_2 and silica alumina, do not cause ethylene polymerization at r.t. but are able to polymerize propene and isobutene. Moreover, very strongly acidic surfaces like HZSM5 zeolite allow polymerization+skeletal isomerization of olefins, like 1-butene with the production of polyisobutene [20]. A Brønsted acidity scale for solid acids measured using this method is reported in Table 7, where a comparison of the three methods we proposed can be made. It seems evident that the olefin polymerization method can discriminate between very strong Brønsted acid solids, while the H-bonding method can discriminate between weak Brønsted acid solids.

References

[1] E.P. Parry, J. Catal. 2 (1963) 371.
[2] N.E. Trietyakov, V.N. Filimonov, Kinet. Katal. 14 (1973) 803.
[3] H. Knözinger, Adv. Catal. 25 (1976) 184.
[4] W.L. Jorgensen, L. Salem, The Organic Chemist's Book of Orbitals, Academic, New York, 1973.
[5] G. Pacchioni, G. Cogliandro, P.S. Bagus, Surf. Sci. 255 (1991) 344.
[6] G. Busca, Langmuir 2 (1986) 577; G. Busca, G. Ramis, V. Lorenzelli, J. Mol. Catal. 50 (1989) 231; G. Ramis, C. Cristiani, A.S. Elmi, P.L. Villa, G.Busca, J. Mol. Catal. 61 (1990) 319.
[7] A. Zecchina, D. Scarano, S. Bordiga, G. Ricchiardi, G. Spoto, F. Geobaldo, Catal. Today 27 (1996) 403.
[8] R. Eisenberg, D.E. Hendriksen, Advan Catal. 28 (1979) 79.
[9] T.R. Hughes, H.M. White, J. Phys. Chem. 71 (1967) 2192.
[10] G. Ramis, G. Busca, J. Mol. Struct. 193 (1989) 93.
[11] A.A. Tsyganenko, D.V. Pozdnyakov, V.N. Filimonov, J. Mol. Struct. 29 (1975) 299.
[12] G. Ramis, Li Yi , G. Busca, M. Turco, E. Kotur, R.J. Willey, J. Catal. 157 (1995) 523.
[13] G. Ramis, G. Busca, C. Cristiani, L. Lietti, P. Forzatti, F. Bregani, Langmuir 8 (1992) 1744.
[14] C.U.I. Odenbrand, J.G.M. Brandin, G. Busca, J. Catal. 135 (1992) 505.
[15] G. Busca, G. Centi, F. Trifirò, J. Am. Chem. Soc. 107 (1985) 7757.
[16] C. Laurence, M. Barthelot, Spectrochim. Acta 34A (1978) 1127.
[17] G. Ramis, G. Busca, V. Lorenzelli, A. La Ginestra, P. Galli, M.A. Massucci, J. Chem. Soc. Dalton Trans. (1988) 881.
[18] A. Chambellan, T. Chevreau, S. Khabtou, M. Marzin, J.C. Lavalley, Zeolites 12 (1992) 306.
[19] S. Odinokov, A.A. Mashkovsky, V.P. Glazunov, A.V. Iogansen, B.V. Rassadin, Spectrochim. Acta 32A (1976) 1355.
[20] G. Ramis, G. Busca, V. Lorenzelli, in: A. Zecchina, G. Costa, C. Morterra (Eds.), Structure and Reactivity of Surfaces, Elsevier, Amsterdam, 1989, p. 777.
[21] M. Trombetta, G. Busca, S.A. Rossini, V. Piccoli, U. Cornaro, J. Catal. 168 (1997) 349.